Supplementary Materials

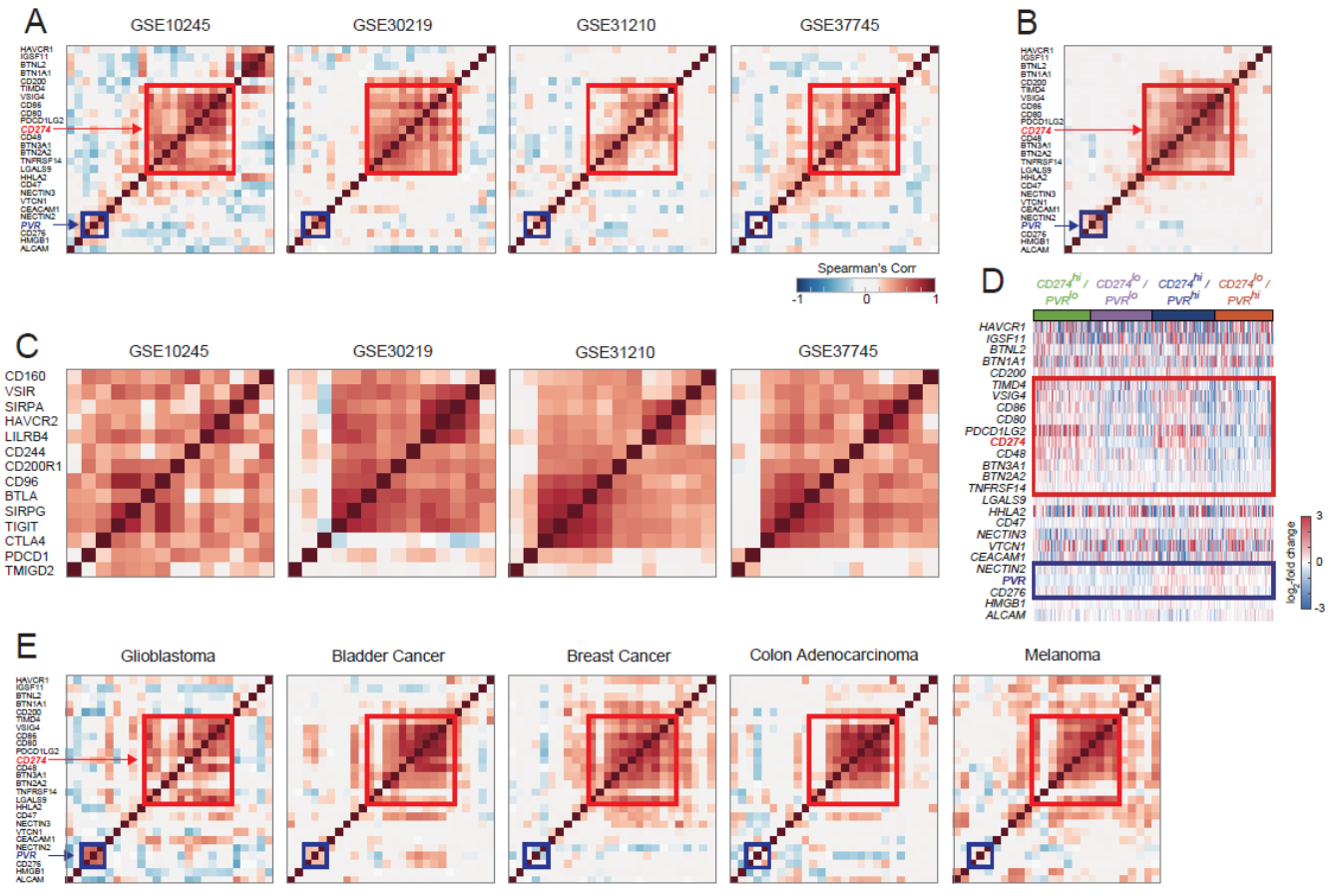

Figure S1. Co-expression patterns of ICLs and ICRs in various cancers. (**A**)-(**C**), Correlation patterns of ICLs (**A**) and ICRs (**C**) in gene expression omnibus database (GSE10245, GSE30219, GSE31210, and GSE37745), and representative correlation pattern of ICLs in lung adenocarcinoma datasets (**B**). The heat maps show the Spearman's correlation coefficients of all the pairs of ICLs (or ICRs) in the order of the ICLs (or ICRs) determined from hierarchical clustering in Fig. 1A (or 1B). In each heat map, the red and blue colors represent the positive and negative correlations among the ICLs or ICRs. The red and blue branches in the dendrogram represent the PD-L1 (CD274, red box) and PVR (blue box) clusters, respectively. (**D**), Gene expression patterns of the ICLs in four patient groups ($CD274_{hi}/PVR_{lo}$, $CD274_{lo}/PVR_{lo}$, $CD274_{hi}$ /PVR_{hi} and $CD274_{lo}/PVR_{hi}$) in the GSE31210 dataset. Red and blue colors represent increased and decreased expression levels of each ICL, respectively, with respect to its median expression level. The color bar denotes the gradient of log2-fold-changes of expression levels in individual samples with respect to its median expression level. (**E**), Correlation patterns of 27 ICLs in five TCGA major cancers: glioblastoma, bladder, and breast cancer, colon adenocarcinoma, and melanoma.

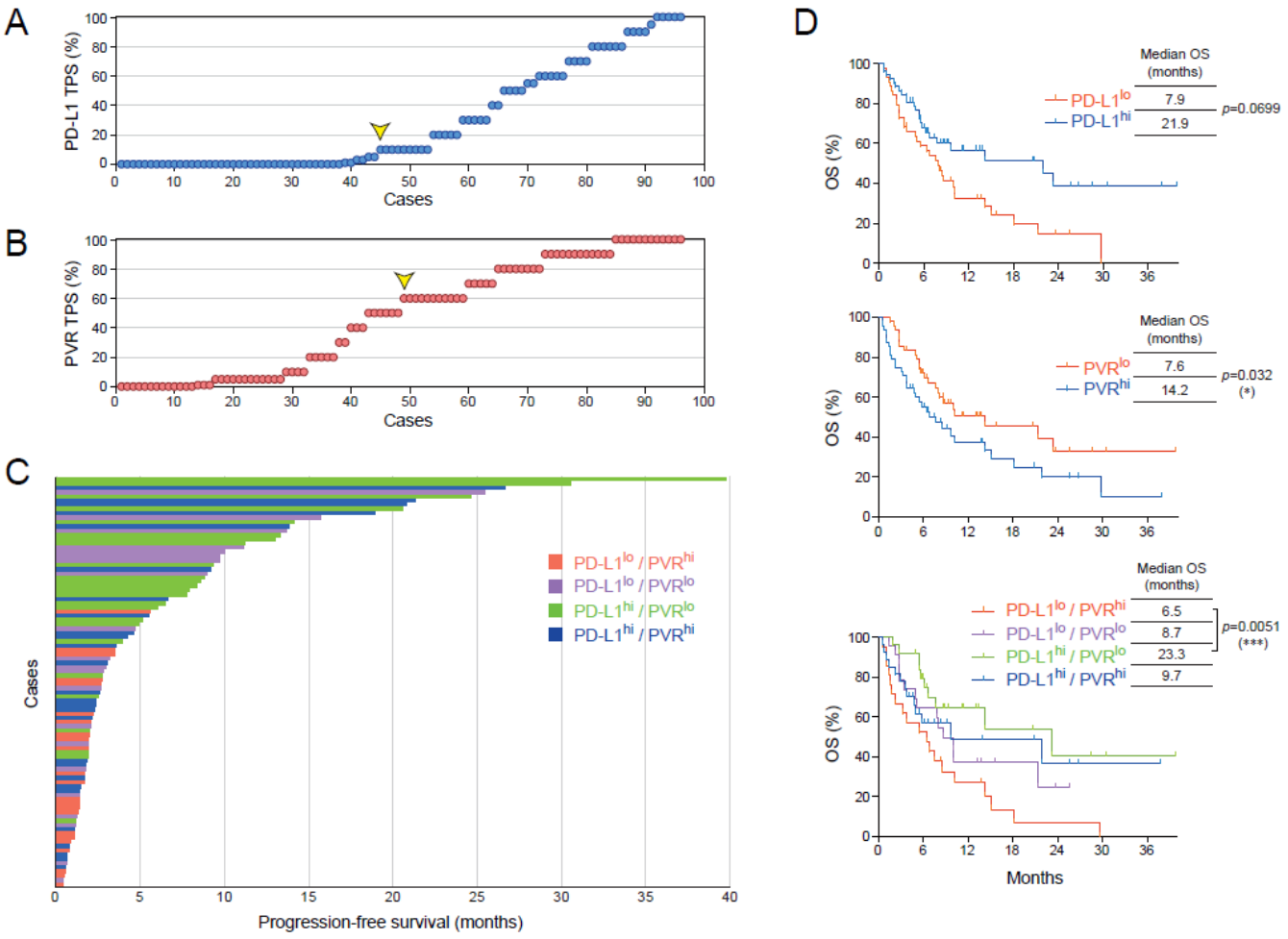

Figure S2. Low PVR expression enriches responders to PD-1 blockade when combined with PD-L1 expression in 96 NSCLC patients of discovery cohort. (A) and (B), Distribution of PD-L1 (A) and PVR (B) TPS of each tumor from individual patients with NSCLC, assessed by IHC staining. (C), Swimmer plot depicting the PFS of individual NSCLC patients enrolled in anti-PD-1 therapy. (D), Kaplan-Meier plots of overall survival (OS) by PD-L1 or/and PVR expression above or below the median for anti-PD-1 therapy. *$p < 0.05$; ***$p < 0.001$ by multivariate Wilcoxon with multiple comparison test for four groups of survival time.

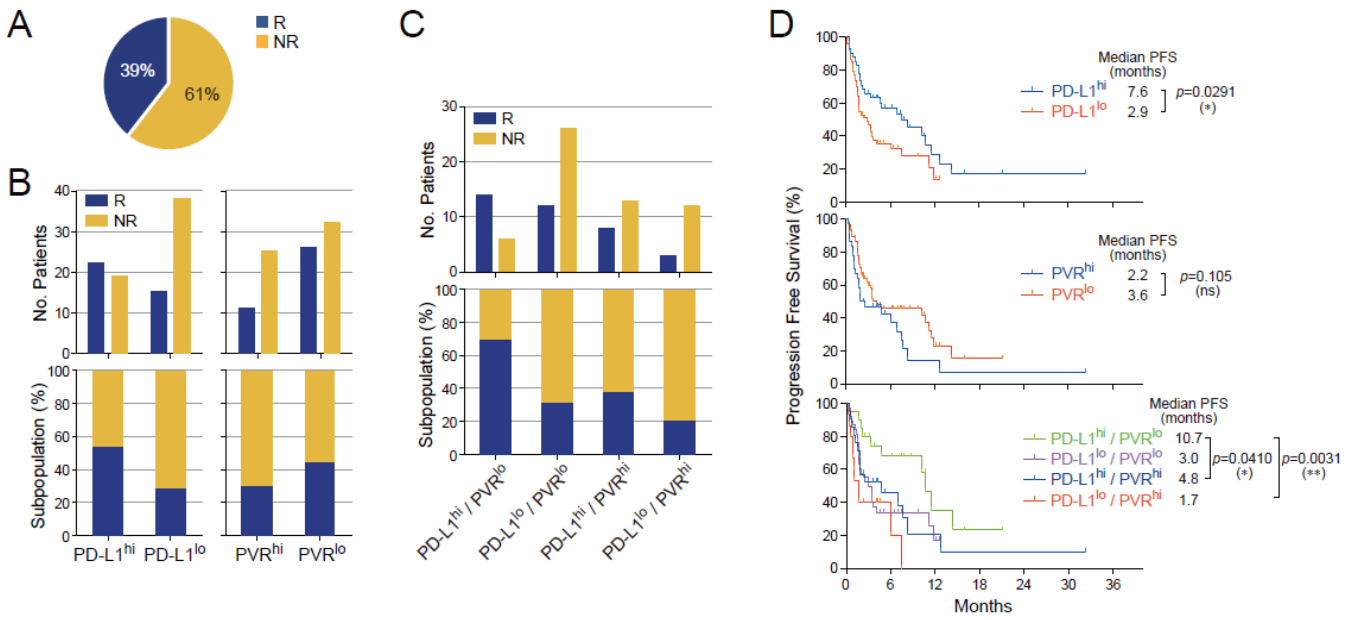

Figure S3. Combinatorial expression pattern of PD-L1 and PVR predicts responders to PD-1 blockade with a better accuracy than PD-L1 expression alone in 94 NSCLC patients of validation cohort. (**A**), Pie chart depicting the overall objective response rate (ORR) of 94 NSCLC patients enrolled in PD-1 blockade. (**B**) and (**C**), Number of responding or non-responding patients for PD-1 blockade by PD-L1 or/and PVR above or below the median and ORR calculated by the number of responding or non-responding patients. Blue, responders (R). Yellow, non-responders (NR). (**D**), Kaplan-Meier plots of progression-free survival (PFS) by PD-L1 or/and PVR expression above or below the median for PD-1 blockade. *$p < 0.05$; **$p < 0.01$ by multivariate Wilcoxon with multiple comparison test for four groups of survival time.

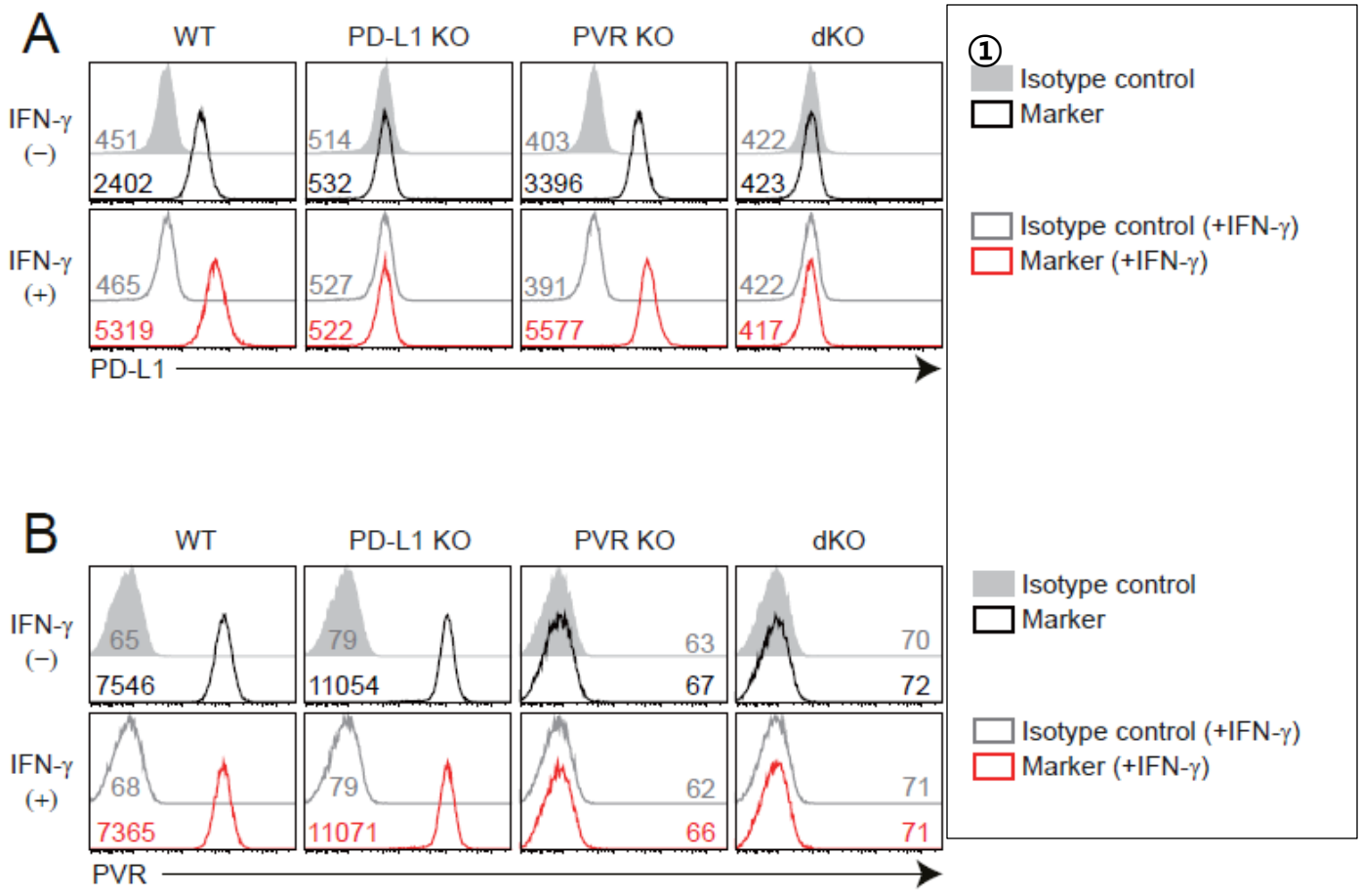

Figure S4. IFN-γ responsiveness of KO cell lines. (**A**) and (**B**), The expression of PD-L1 (**A**) and PVR (**B**) in each KO cell line was determined by flow cytometry. The absence of PD-L1 was confirmed by treatment with IFN-γ (10 ng/ml) for 24 h. The mean fluorescence intensity (MFI) values of PD-L1 or PVR and their isotypes are depicted in the FACS plots. Data are representative of two independent experiments.

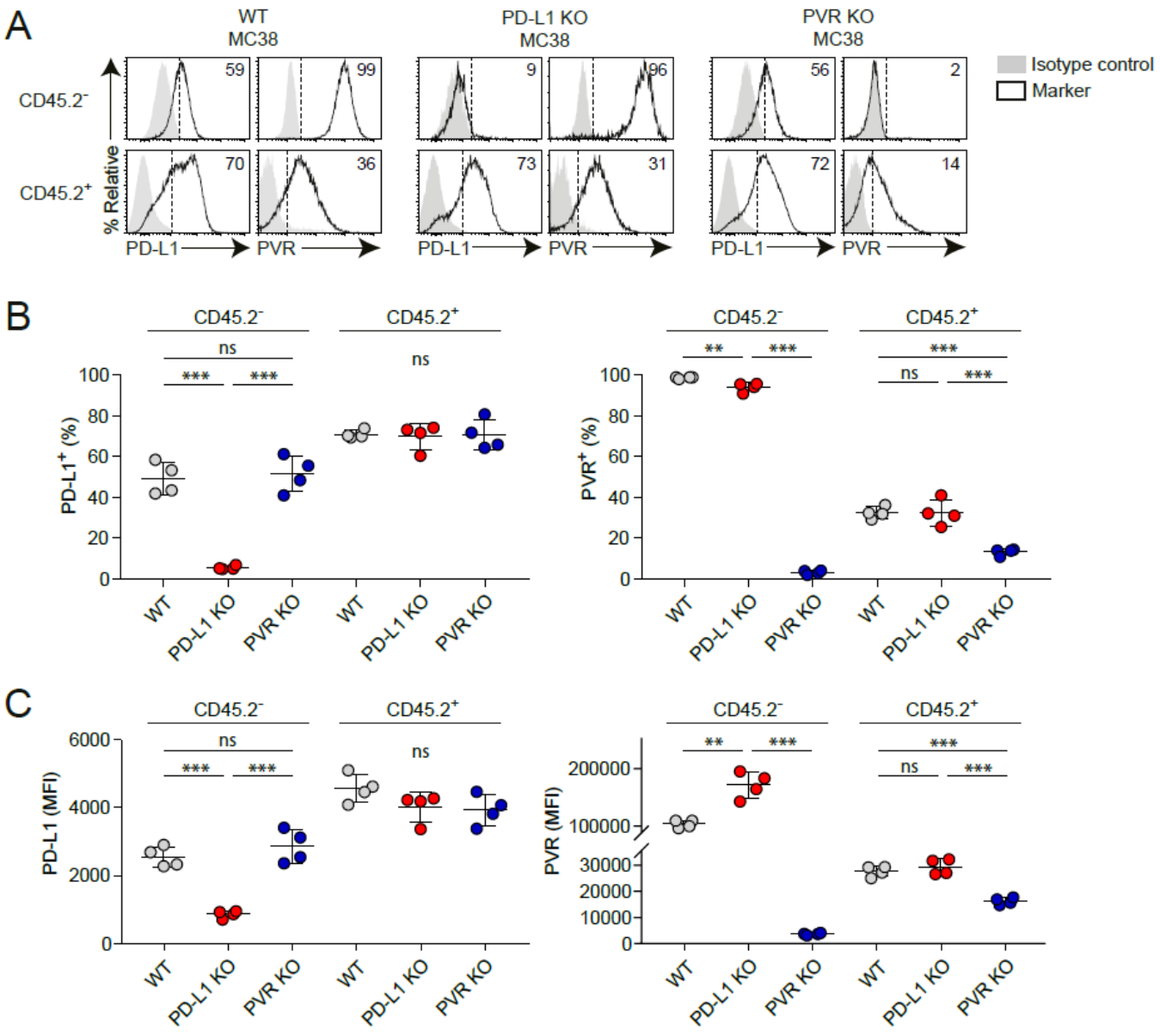

Figure S5. PD-L1 and PVR expression by CD45.2- and CD45.2+ cells in tumor microenvironment. (A)-(C), Each tumor was generated by injecting WT, PD-L1 KO, or PVR KO MC38 tumor cells into mice (n=4 per group). Once established (100~200 mm^3), PD-L1 and PVR expressions by CD45.2- cells and CD45.2+ cells in each tumor were quantified by flow cytometry. Representative histogram shown with mean percentage of expression (A) and proportion of PD-L1 or PVR-expressing cells in CD45.2- cells and CD45.2+ cells from each tumor type (B). The MFIs of PD-L1 or PVR-expressing cells were also summarized (C). The data are represented as the mean ± SEM and are representative of two independent experiments. $^{**}p < 0.01$; $^{***}p < 0.001$ by 1-way ANOVA with Tukey's multiple comparisons test.

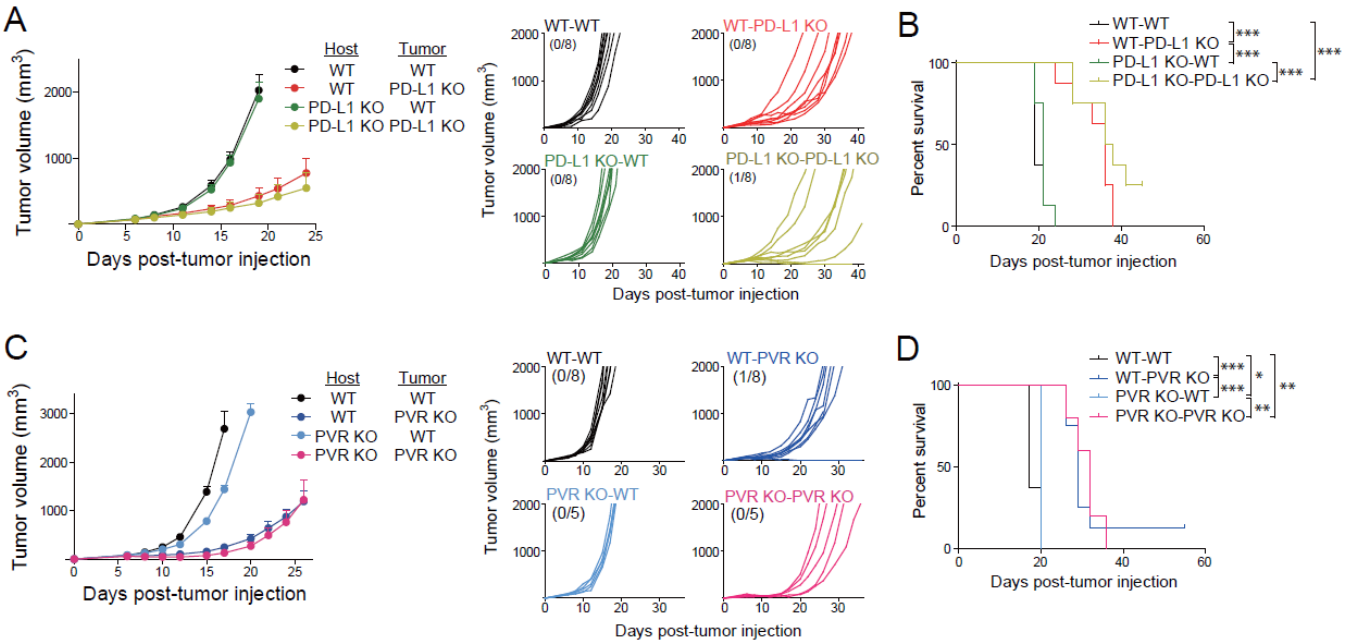

Figure S6. Tumor-expressing PVR or PD-L1 is more critical to tumor-immune escape and tumor progression than host-expressing. (**A**) and (**B**), WT or PD-L1 KO MC38 tumor cells (1×10^5 cells each, n=8 per group) were subcutaneously injected into WT B6 or PD-L1 KO mice. The tumor growth (**A**) and survival (**B**) of each tumor-bearing mouse. (**C**) and (**D**), WT or PVR KO MC38 tumor cells (1×10^5 cells each, n=8 or n=5 per group, as noted in parentheses) were subcutaneously injected into WT B6 or PVR KO mice. The tumor growth (**C**) and survival (**D**) of each tumor-bearing mouse. The numbers in parentheses denote the tumor-free mice/total mice after transplantation. The data are represented as the mean ± SEM and are representative of two independent experiments. *$p < 0.05$; **$p < 0.01$; ***$p < 0.001$ by multivariate Wilcoxon with multiple comparison test for four groups of survival time.

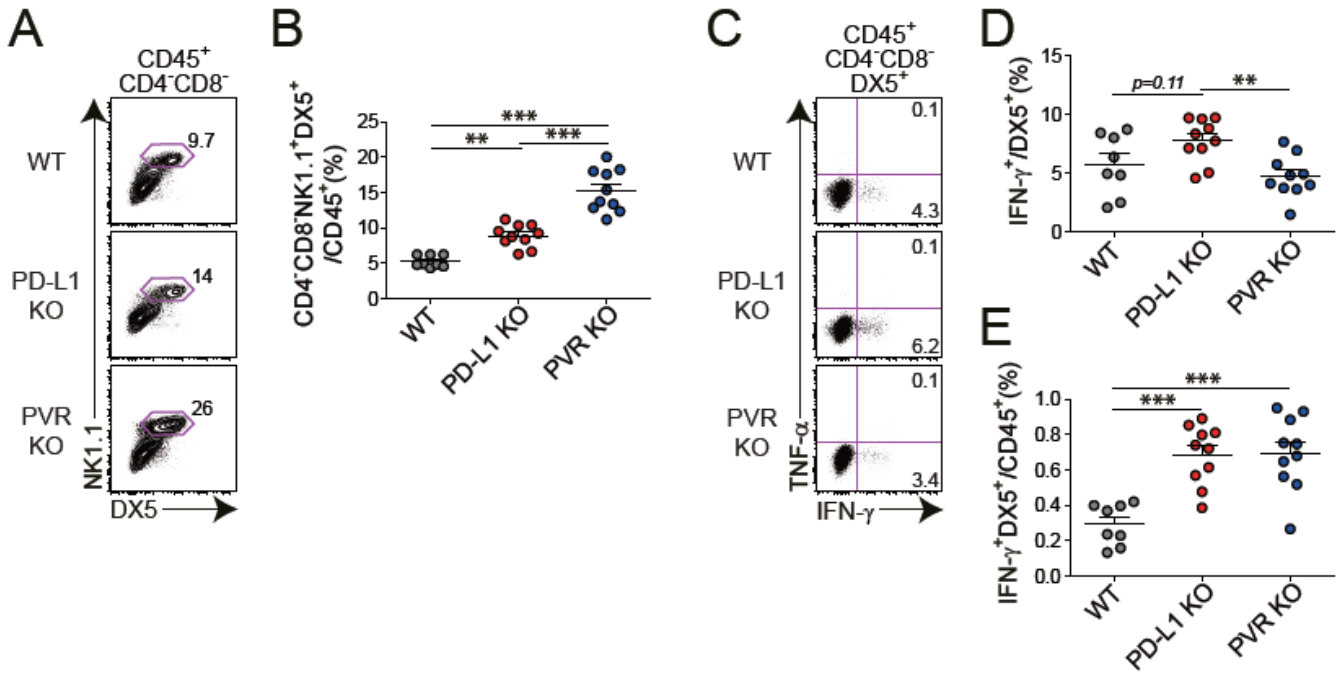

Figure S7. PVR and PD-L1 modulates NK cells in parallel with CD8+ T cells in tumor immune microenvironment. Once established (100~200 mm^3), each tumor harvested from WT (black, *n*=8), PD-L1 KO (red, *n*=10), or PVR KO (blue, *n*=10) MC38-bearing mice was analyzed by flow cytometry. NK cells were analyzed by flow cytometry in the same experimental condition as Fig. 3D-3L. (**A**), Representative FACS plots of NK cell infiltration in tumors. (**B**), Frequency of NK cells (CD4-CD8-DX5+) among CD45+ cells in tumors. (**C**)-(**E**), Representative FACS plots (**C**) and the frequency of IFN-γ+ cells among NK cells (**D**) and IFN-γ+ CD8+ T cells (**E**) in each tumor type. The data are represented as the mean ± SEM with each dot indicating one mouse. Data are representative of two independent experiments. $^{**}p < 0.01$; $^{***}p < 0.001$ by 1-way ANOVA with Tukey's multiple comparisons test.

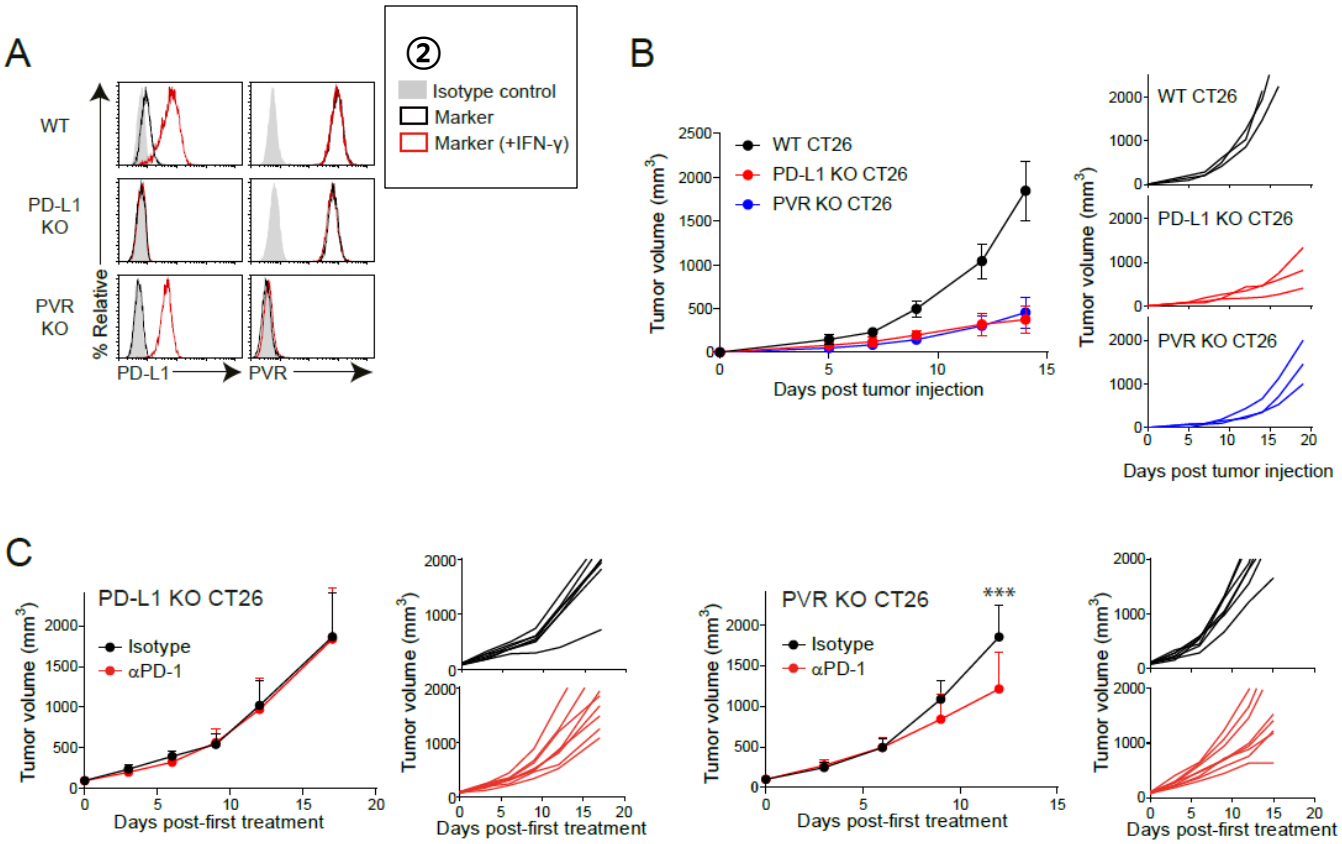

Figure S8. Differential sensitivity for PD-1 blockade depending on the expression of PD-L1 and PVR in CT26 tumor. (**A**), PD-L1 KO and PVR KO CT26 tumor cells were generated from parental WT CT26 using the CRISPR/Cas9 system, and expression of PD-L1 and PVR was assessed by flow cytometry. Before analysis, cells were incubated for 24h in the presence (red) or absence (black) of IFN-γ (10ng/ml). (B), BALB/c mice were injected subcutaneously with WT(black), PD-L1 KO (red), or PVR KO (blue) CT26 tumor cells **(③+ (*n*=3 per group))** Tumor sizes were measured at the indicated **time points (C), Once established (80-120 mm3), mice with PD-L1 KO (*n*=8) or PVR KO (*n*=8). (④ →time points. (C), Once established (80-120 mm3), mice with PD-L1 KO (*n*=8) or PVR KO (*n*=8))** CT26 tumor were treated intraperitoneally with 200 μg of isotype control (black) or anti-PD-1 (red) per time (total 5 times, every three days). Tumor sizes were measured at the indicated time points after anti-PD-1 therapy. The data are represented as the mean ± SEM. Data are representative of two independent experiments with $n \geq 8$ mice in each experiment. ***$p < 0.001$ with 2-way ANOVA with Sidak's multiple comparisons test

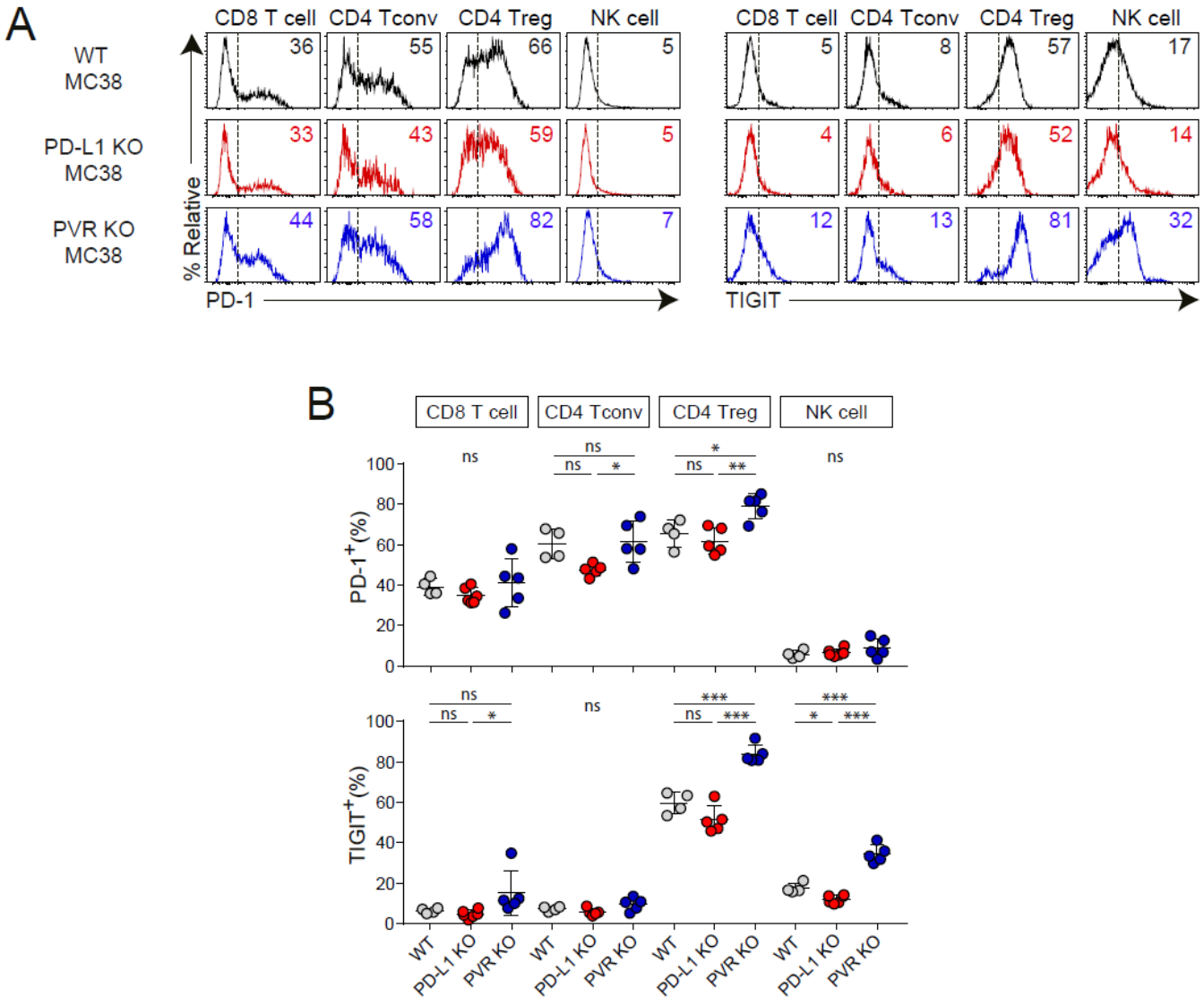

Figure S9. PD-1 and TIGIT expression on various subsets of tumor-infiltrating lymphocytes in tumor microenvironment depending on PD-L1 or PVR expression. Once established (110~130 mm^3), each tumor harvested from WT (black, *n*=4), PD-L1 KO (red, *n*=5), or PVR KO (blue, *n*=5) MC38-bearing mice was analyzed by flow cytometry to quantify the expressions of PD-1 and TIGIT on lymphocytes. (**A**), Representative histogram shown with frequency of PD-1+ or TIGIT+ cells in each subset of lymphocytes. (**B**), The data in (**A**) was summarized as the mean ± SEM with each dot indicating one mouse. Data are representative of two independent experiments. *$p < 0.05$; **$p < 0.01$; ***$p < 0.001$ by 1-way ANOVA with Tukey's multiple comparisons test

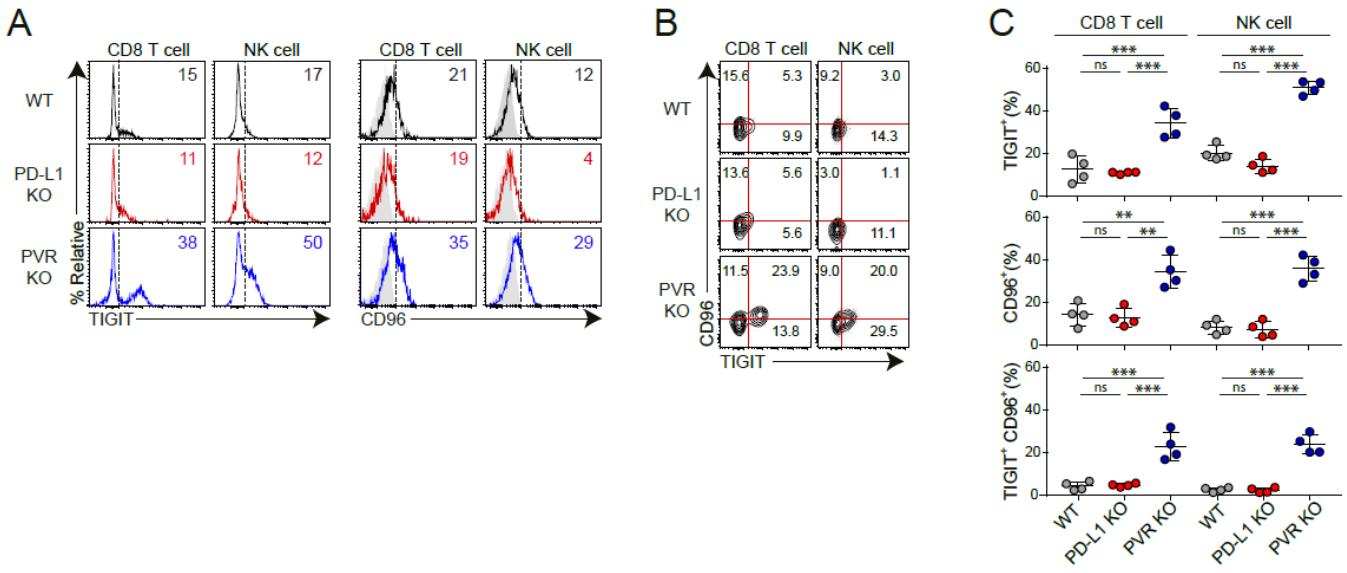

96

97 **Figure S10. TIGIT and CD96 expression are upregulated on PVR KO tumor-infiltrating**
98 **lymphocytes.** Once established (140~160 mm^3), each tumor harvested from WT (black, *n*=4), PD-L1 KO
99 (red, *n*=4), or PVR KO (blue, *n*=4) MC38-bearing mice was analyzed by flow cytometry to quantify the
100 expressions of TIGIT and CD96 on either $CD8^+$ T cells or NK cells. (**A**)-(**B**), Representative histograms
101 and contour plots showing $TIGIT^+$, $CD96^+$, or $TIGIT^+$ $CD96^+$ cells among $CD8^+$ T cells or NK cells in
102 each tumor type. (**C**), Frequency of $TIGIT^+$, $CD96^+$, and $TIGIT^+$ $CD96^+$ cells among $CD8^+$ T cells or NK
103 cells in each tumor type was summarized as the mean ± SEM with each dot indicating one mouse. Data
104 are representative of two independent experiments. $^{**}p < 0.01$; $^{***}p < 0.001$ by 1-way ANOVA with
105 Tukey's multiple comparisons test.

106

Table S1. Comparison of baseline patient characteristics between discovery and validation set

Variables	Discovery set (N=96)	Validation set (N=94)	P-value
Age (year)			0.774
<65	49 (51%)	50 (53.2%)	
≥65	47 (49%)	44 (46.8%)	
Gender			0.623
Male	69 (71.9%)	71 (75.5%)	
Female	27 (28.1%)	23 (24.5%)	
Smoking status			0.334
Never smoker	30 (31.2%)	23 (24.5%)	
Ever smoker	66 (68.8%)	71 (75.5%)	
Histology			0.880
Adenocarcinoma	62 (64.6%)	62 (66.0%)	
Squamous carcinoma	34 (35.4%)	32 (34.0%)	
EGFR status			0.820
Wild-type	86 (89.6%)	83 (88.3%)	
Mutant	10 (10.4%)[A]	11 (11.7%)[B]	
ALK status			0.988
Wild-type	95 (99.0%)	93 (98.9%)	
Rearrangement	1 (1.0%)	1 (1.1%)	
Immunotherapeutic agent			0.998
Nivolumab	67 (69.8%)	68 (72.3%)	
Pembrolizumab	26 (27.1%)	23 (24.5%)	
Atezolizumab	3 (3.1%)	3 (3.2%)	
Response to blockade			0.765
Responder[C]	35 (36.5%)	37 (60.6%)	
Non-responder	61 (63.5%)	57 (39.4%)	

[A]EGFR mutant type in discovery set: Exon19deletion (n=5), Exon19deletion/T790M (n=1), Exon 21 L858R (n=4), and Exon18 S768I (n=1)

[B]EGFR mutant type in validation set: Exon19deletion (n=3), Exon19deletion/T790M (n=3), Exon 21 L858R (n=3), and Exon18 S768I (n=1), Exon20 insertion (n=1)

[C]Responder: The patients who show partial response or stable disease (≥6months)

Table S2. Patient characteristics according to PD-L1/PVR expression in validation set

Variables	No. of samples	PD-L1/PVR expression				P-value
		lo/hi	lo/lo	hi/lo	hi/hi	
Age (year)						
<65	50 (53.2%)	7 (7.4%)	21 (22.3%)	7 (7.4%)	15 (16.0%)	0.190
≥65	44 (46.8%)	7 (7.4%)	17 (18.1%)	13 (13.8%)	7 (7.4%)	
Gender						
Male	71 (75.5%)	10 (10.6%)	29 (30.9%)	14 (14.9%)	18 (19.1%)	0.815
Female	23 (24.5%)	4 (4.3%)	9 (9.6%)	6 (6.4%)	4 (4.3%)	
Smoking status						
Never smoker	23 (24.5%)	3 (3.2%)	11 (11.7%)	6 (6.4%)	3 (3.2%)	0.530
Ever smoker	71 (75.5%)	11 (11.7%)	27 (28.7%)	14 (14.9%)	19 (20.2%)	
Histology						
Adenocarcinoma	62 (66.0%)	12 (12.8%)	24 (25.5%)	11 (11.7%)	17 (18.1%)	0.052
Squamous carcinoma	32 (34.0%)	2 (2.1%)	14 (14.9%)	9 (9.6%)	5 (5.3%)	
EGFR status						
Wild-type	83 (88.3%)	12 (12.8%)	35 (37.2%)	18 (19.1%)	18 (19.1%)	0.665
Mutant[A]	11 (11.7%)	2 (2.1%)	3 (3.2%)	2 (2.1%)	4 (4.3%)	
ALK status						
Wild-type	93 (98.9%)	14 (14.9%)	37 (39.4%)	20 (21.3%)	22 (23.4%)	0.685
Rearrangement	1 (1.1%)	0 (0%)	1 (1.1%)	0 (0%)	0 (0%)	
Immunotherapeutic agent						
Nivolumab	68 (72.3%)	12 (12.8%)	34 (36.2%)	11 (11.7%)	11 (11.7%)	0.003
Pembrolizumab	23 (24.5%)	2 (2.1%)	3 (3.2%)	7 (7.4%)	11 (11.7%)	
Atezolizumab	3 (3.2%)	0 (0%)	1(1.1%)	2 (2.1%)	0 (0%)	
Response to PD-1 blockade						
Responder[B]	37 (60.6%)	2 (2.1%)	12 (12.8%)	14 (14.9%)	9 (9.6%)	0.06
Non-responder	57 (39.4%)	12 (12.8%)	26 (27.7%)	6 (6.4%)	13 (13.8%)	

[A]EGFR mutant type in validation set: Exon19deletion (n=3), Exon19deletion/T790M (n=3), Exon 21 L858R (n=3), and Exon18 S768I (n=1), Exon20 insertion (n=1)

[B]Responder: The patients who show partial response or stable disease (≥6 months)

Table S3. Univariate and multivariate factors affecting the response to anti-PD-1 therapy in validation set

Variable	Category	Univariate survival analysis			Multivariate survival analysis		
		HR	95% CI	P-value	AHR	95% CI	P-value
Age (years)	≥65 vs. <65	0.741	0.450-1.219	0.238	0.833	0.485-1.430	0.508
Sex	Female vs. male	1.872	1.081-3.224	0.025	2.885	0.632-13.168	0.171
Smoking	Smoker vs. never smoker	0.583	0.338-1.008	0.053	1.278	0.291-5.615	0.746
Histology	Squamous vs. non-squamous	0.691	0.405-1.179	0.175	1.080	0.580-2.012	0.808
EGFR status	Mutant vs. wild-type	1.420	0.691-2.919	0.340	0.877	0.347-2.217	0.782
Treatment line	≥ 3rd line vs. 2nd line	1.147	0.690-1.906	0.597	0.919	0.504-1.675	0.781
PD-L1[A]	≥10% vs. <10%	0.559	0.332-0.940	0.028	0.512	0.298-0.878	0.015
PVR[A]	≥60% vs. <60%	1.568	0.949-2.592	0.079	1.792	0.995-3.227	0.052
PD-L1/PVR status[A]	PD-L1^{+}/PVR^{-} vs. others	0.771	0.585-1.017	0.066	0.370	0.182-0.755	0.006

Abbreviations: HR, hazard ratio; AHR, adjusted hazard ratio; CI, confidence interval

[A]In multivariate analysis, one factor of PD-L1, PVR, and PD-L1/PVR is included for analysis.